The solubility of carbon dioxide in aqueous N-methyldiethanolamine solutions

Huttenhuis, P. J. G.; Agrawal, N. J.; Solbraa, E.; Versteeg, G. F.

Published in:
Fluid Phase Equilibria

DOI:
10.1016/j.fluid.2007.10.020

Publication date:
2008

Available online at www.sciencedirect.com
ScienceDirect
Fluid Phase Equilibria 264 (2008) 99–112
FLUID PHASE EQUILIBRIA
www.elsevier.com/locate/fluid

The solubility of carbon dioxide in aqueous *N*-methyldiethanolamine solutions

P.J.G. Huttenhuis [a,*], N.J. Agrawal [a], E. Solbraa [b], G.F. Versteeg [a]

[a] *Procede Group B.V., P.O. Box 328, 7500 AH, Enschede, The Netherlands*
[b] *Statoil ASA, Research and Technology, Rotvoll, 7005 Trondheim, Norway*

Received 30 May 2007; received in revised form 26 October 2007; accepted 29 October 2007
Available online 13 November 2007

Abstract

In this study the electrolyte equation of state as proposed by Solbraa [E. Solbraa, Equilibrium and non-equilibrium thermodynamics of natural gas processing, Ph.D. thesis Norwegian University of Science and Technology, 2002] was systematically studied and improved to describe the solubility of carbon dioxide in aqueous solutions of *N*-methyldiethanolamine quantitatively. In this electrolyte equation of state approach both the vapour phase and the liquid phase are described with an equation of state. The molecular part of the equation is based on Schwarzentruber's [J. Scharzentruber, H. Renon, S. Watanasiri, Fluid Phase Equilib. 52 (1989) 127–134] modification of the Redlich-Kwong equation of state with the Huron–Vidal mixing rule [M.J. Huron, J. Vidal, Fluid Phase Equilib. 3 (1979) 255–271]. Three ionic terms are added to this equation—a short-range ionic term, a long-range ionic term (MSA) and a Born term. The thermodynamic model has the advantage that it reduces to a standard cubic equation of state if no ions are present in the solution, and that publicly available interaction parameters used in the Huron–Vidal mixing rule can be utilized. In this work binary molecular- and ionic interaction parameters were studied and optimized. With the updated model it was possible to describe both low- and high pressure vapour–liquid-equilibrium for the MDEA–H_2O–CO_2–CH_4 system satisfactorily.

Keywords: Carbon dioxide; *N*-Methyldiethanolamine; Solubility; Electrolyte equation of state; Gas treating

1. Introduction

Acid components like CO_2 and H_2S are normally (selectively) removed to a certain extent in natural and industrial gas streams. The most commonly used systems for this process are the alkanolamine solvents, where the acid components are removed with a reactive absorption liquid, i.e. an aqueous alkanolamine solution. The acid gas will partly be converted to non-volatile ionic species by the basic amine and partly be dissolved physically in the liquid solution. For a robust design of such process systems the acid gas solubility (VLE data), the reaction rate and the mass transfer properties should be known accurately. MDEA is a relatively cheap chemical, it is stable and the loaded solvent has a relatively low heat of regeneration. In this work experimental solubility data available in the literature are interpreted with an electrolyte equation of state (E-EOS) model for the system MDEA–H_2O–CO_2–CH_4. MDEA is a commonly used alkanolamine in the gas treating industry. With the E-EOS thermodynamic model all molecular and ionic concentrations for the MDEA–H_2O–CO_2–CH_4 can be calculated at chemical equilibrium conditions. In the literature many models are presented to predict the acid gas solubility in alkanolamine systems. These models can be divided into three categories:

- Empirical models like Kent–Eisenberg [2]. The Kent–Eisenberg model is based on chemical reaction equilibrium in the liquid phase. All activity and fugacity coefficients are assumed to be equal to unity and both the equilibrium constant of the amine protonation reaction and the carbamate formation reaction are, respectively, used as fitting parameters in the model, to match the model with the experimental data. Extrapolation applicability outside the validity range is very limited. This model is commonly

* Corresponding author. Tel.: +31 489 5340; fax: +31 489 5399.
E-mail address: patrick.huttenhuis@procede.nl (P.J.G. Huttenhuis).

0378-3812/$ – see front matter © 2007 Elsevier B.V. All rights reserved.
doi:10.1016/j.fluid.2007.10.020

used by process engineers because complexity and required computational effort are relatively low.
- Excess Gibbs energy models. In these models, a term for electrostatic forces caused by the presence of ions in the liquid phase is added to the molecular Gibbs free energy models like NRTL. This additional term is normally based on the Debye and Hückel expression. Approaches based on excess Gibbs energy are presented by: Desmukh–Mather [3], Clegg–Pitzer [4] and Austgen et al. [5]. The vapour phase is predicted with a suitable equation of state.
- Equation of state models (EOS). In this approach both the liquid and the vapour phase are represented with an equation of state. Additional electrolyte terms for the forces resulting from the presence of ions are added to the molecular equation of state. These kinds of models are rather new for the prediction of acid gas solubility in alkanolamine solutions (Fürst and Planche [6], Solbraa [7], Derks et al. [8]).

A more detailed comparison of these thermodynamic models used in the gas treating industry is presented by Huttenhuis and Versteeg [10].

In this work the experimental data will be interpreted with an electrolyte equation of state. This model selection is based on the following motivation:

- EOS models apply the same description for liquid and gas phase.
- The model should be able to model gas, condensate and amine equilibrium (VLLE) in a consistent way.
- Extrapolation capabilities of the model seem feasible.
- Prediction at high pressures, typically found in the natural gas industry, is expected to be more reliable compared to other thermodynamic models.
- The model can be extended to systems where different kind of inert components like hydrocarbons are present.
- The model reduces to a standard cubic equation of state if no ions are present in the solution, and by that enables consistent overall natural gas process simulation.

2. Description of electrolyte equation of state model

2.1. General

The experimental results are interpreted with an electrolyte equation of state model (E-EOS), originally proposed by Fürst and Renon [9]. In this model the same equations, based on an equation of state, are used for both the liquid and vapour phase. It is expected that these EOS models will be superior in representing the thermodynamic properties outside the experimentally tested region. Moreover it is expected that the speciation of the components occurring in the liquid phase can be calculated more reliable. An accurate prediction of the speciation is important for the mass transfer calculations. Moreover, the solubility of physically dissolved hydrocarbons (i.e. methane) can be calculated in a thermodynamic consistent way. This hydrocarbon solubility is an important parameter for the correct design of high pressure gas treating equipment.

The basic equation of the model is based on an Helmholtz free energy expression. The Helmholtz energy is given by the equation below and is defined as the sum of five contributions:

$$\left(\frac{A^{\mathrm{R}}}{RT}\right) = \overset{1}{\left(\frac{A^{\mathrm{R}}}{RT}\right)}_{\mathrm{RF}} + \overset{2}{\left(\frac{A^{\mathrm{R}}}{RT}\right)}_{\mathrm{SR1}} + \overset{3}{\left(\frac{A^{\mathrm{R}}}{RT}\right)}_{\mathrm{SR2}} + \overset{4}{\left(\frac{A^{\mathrm{R}}}{RT}\right)}_{\mathrm{LR}} + \overset{5}{\left(\frac{A^{\mathrm{R}}}{RT}\right)}_{\mathrm{BORN}} \quad (1)$$

The first two (molecular) terms are the terms obtained from the used (molecular) equation of state and the other terms are added due to the presence of electrolytes in the system.

In Fig. 1 an overview is given of which types of interaction parameters in the E-EOS model for the system MDEA–CO_2–H_2O–CH_4 are used and how these parameters are determined from the corresponding subsystems. At the bottom level the system independent pure component molecular and ionic parameters are presented. The binary molecular interaction parameters were determined from the binary systems. The binary ionic interaction parameters were determined by fitting them to the experimental VLE-database derived from open literature publications for the systems CO_2–MDEA–H_2O and CO_2–MDEA–H_2O–CH_4. More details about the model and the relevant parameters are described in the following sections.

2.2. Pure component model

The first term of the Helmholtz contributions accounts for the molecular repulsive forces (RF) and the second term for the short-range (attractive) interactions (SR1). The molecular part of the model was based on a cubic equation of state (Schwarzentruber's [1] modification of the Redlich-Kwong-Soave EOS (ScRK-EOS) with a Huron–Vidal [11] mixing rule).

This ScRK-EOS is described by the following formulae:

$$P = \frac{RT}{v-b} - \frac{a}{v(v+b)} \quad (2)$$

$$a = \frac{1}{9(2^{1/3}-1)}\frac{(RT_{\mathrm{C}})^2}{P_{\mathrm{C}}}\alpha(T_{\mathrm{R}}), \qquad b = \frac{(2^{1/3}-1)}{3}\frac{RT_{\mathrm{C}}}{P_{\mathrm{C}}},$$

$$\alpha(T_{\mathrm{R}}) = \{1+m(\omega)(1-\sqrt{T_{\mathrm{R}}})-p_1(1-T_{\mathrm{R}})(1+p_2T_{\mathrm{R}}+p_3T_{\mathrm{R}}^2)\}^2$$

$$\text{for} \quad T_{\mathrm{R}} < 1, \qquad \alpha(T_{\mathrm{R}}) = \{\exp[c(1-T_{\mathrm{r}}^{\mathrm{d}})]\}^2 \quad \text{for} \quad T_{\mathrm{R}} > 1$$

$$m(\omega) = 0.48508 + 1.55191\omega - 0.15613\omega^2, \qquad c = 1 - \frac{1}{d},$$

$$d = \frac{1+m(\omega)}{2-p_1(1+p_2+p_3)} \quad (3)$$

Via the application of this Schwarzentruber modification of the RKS equation, it is also possible to calculate the vapour-pressure curve as function of temperature for polar (non-ideal) components. Parameters p_1, p_2 and p_3 are fitting parameters and are determined by regressing the model to the experimental vapour-pressure data.

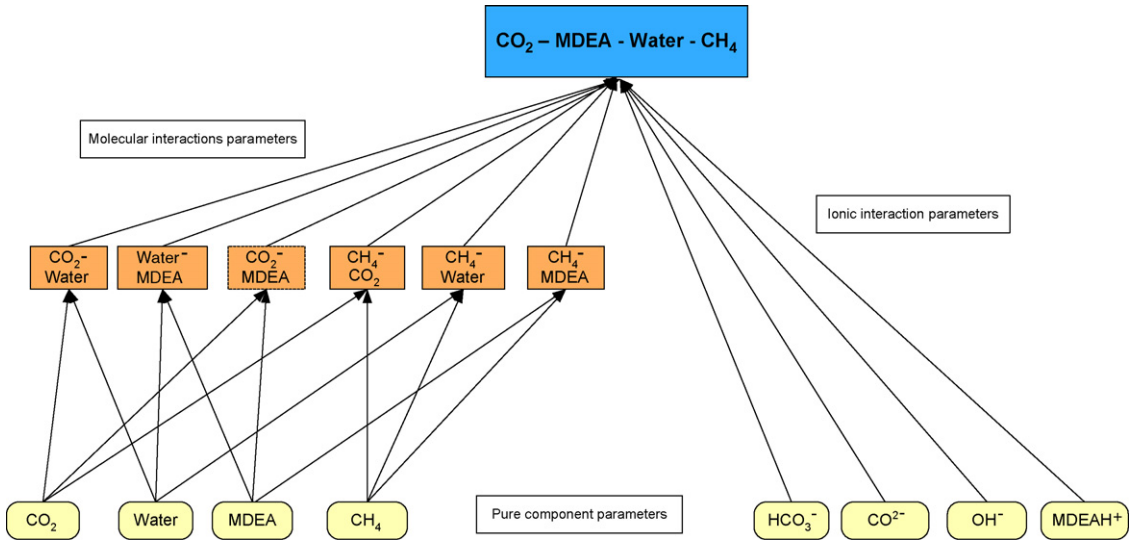

Fig. 1. Overview of the interactions involved in the E-EOS model.

2.3. Mixing rules

The equation of state can also be used to predict physical and thermodynamic properties for mixtures of components. The parameters applicable for pure components like 'a' and 'b' are then determined via a mixing rule. The most simple mixing rule is the linear mixing rule; however, for more accurate model predictions, the mixing rule developed by van der Waals is used:

$$a = \sum_i \sum_i x_i x_j a_{ij}, \quad a_{ij} = \sqrt{a_i a_j}(1 - k_{ij}),$$

$$b = \sum_i \sum_j x_i x_j b_{ij}, \quad b_{ij} = \frac{b_i + b_j}{2} \tag{4}$$

where k_{ij} is a fitting parameter.

In case where components with substantially different structures have to be described the van der Waals mixing rule is not reliable anymore. Huron and Vidal [11] proposed a mixing rule based on excess Gibbs energy models. In this mixing rule the attraction parameter of the mixture (a_{mix}) is calculated in a different way than in the van der Waals method. With this mixing rule better predictions can be obtained for polar, highly non-ideal mixtures:

$$a_{\mathrm{mix}} = b_{\mathrm{mix}} \left(\sum_{i=1}^{n} \left(x_i \frac{a_i}{b_i} \right) - \frac{G^{\mathrm{E}}_{\infty}}{\ln 2} \right) \tag{5}$$

G^{E}_{∞} is the excess Gibbs energy at infinite pressure and can be calculated with a modified NRTL mixing rule:

$$\frac{G^{\mathrm{E}}_{\infty}}{RT} = \sum_{i=1}^{n} x_i \frac{\sum_{j=1}^{n} \tau_{ji} b_j x_j \exp(-\alpha_{ji}\tau_{ji})}{\sum_{k=1}^{n} b_k x_k \exp(-\alpha_{ki}\tau_{ki})} \tag{6}$$

α_{ji} is a non-randomness parameter, which takes into account that the mole fraction of molecule i around molecule j may deviate from the total mole fraction of molecule i in the system.

$$\tau_{ji} = \frac{g_{ji} - g_{ii}}{RT} \tag{7}$$

g_{ji} is an energy parameter caused by the interaction forces between molecule i and j. In the present approach it is assumed that the g-parameters are temperature dependent according to:

$$g_{ij} - g_{jj} = (g'_{ij} - g'_{jj}) + T(g''_{ij} - g''_{jj}),$$
$$g_{ji} - g_{ii} = (g'_{ji} - g'_{ii}) + T(g''_{ji} - g''_{ii}) \tag{8}$$

An additional advantage of this Huron–Vidal mixing rule is that it can easily be converted for non-polar binary systems (i.e. hydrocarbons) to the van der Waals mixing rule by proper choice of parameters. In this work the non-polar binary mixtures are modelled with the van der Waals mixing rule and the polar, non-ideal binary mixtures with the Huron–Vidal mixing rule.

In this model the linear mixing rule is used for the co-volume parameter b_{mix}, while the presence of ions is included:

$$b_{\mathrm{mix}} = \sum_{\mathrm{m}} x_{\mathrm{m}} b_{\mathrm{m}} + \sum_{\mathrm{ion}} x_{\mathrm{ion}} b_{\mathrm{ion}}$$

The molecular co-volume (b_{m}) is calculated from the critical properties and the ionic co-volume (b_{ion}) is calculated from the ionic diameter.

The pure component parameters of the E-EOS model used in this work are presented in Table 1.

2.4. Electrolyte interactions

To describe the interactions caused by the presence of ions in the system the following terms were added to the (molecular) equation of state:

- SR2—a short-range ion–ion interaction term.
- LR—a long-range ion–ion interaction term.
- Born term, a correction term for the standard state of ions.

Table 1
Pure component parameters

	CO_2	MDEA	H_2O	CH_4	HCO_3^-	CO_3^{2-}	$MDEAH^+$	OH^-
M (g mol^{-1})	44.01	119.16	18.02	16.04	61.00	59.98	120.16	17.00
T_C (K)	304.2	677.0	647.3	190.6				
P_C (bar)	74.0	38.8	220.9	45.9				
ω [–]	0.224	1.242	0.344	0.011				
p_1	0.0336	0.5213	0.0740	0.0145				
p_2	−1.3034	−1.1521	−0.9454	1.7953				
p_3	0	−0.0139	−0.6988	−4.2300				
σ (10^{-10} m)[b]	3.94[a]	4.50	2.52[a]	3.17	3.12[a]	3.7[a]	4.50	3.52[a]
$d^{(0)}$[b]	2.00	8.17	−19.29	2.00				
$d^{(1)}$[b]	0	8.989E+03	2.981E+04	0				
$d^{(2)}$[b]	0	0	−1.968E−02	0				
$d^{(3)}$[b]	0	0	1.320E−04	0				
$d^{(4)}$[b]	0	0	−3.110E−07	0				

[a] All parameters are based on Solbraa [7] except those marked with[a], which are based on Vallée et al. [12].
[b] These pure component parameters are used in the electrolyte part of the equation of state as discussed in the next paragraphs.

The short-range ionic interaction term is calculated by the following relation:

$$\left(\frac{A_R}{RT}\right)_{SR2} = -\sum_i \sum_j \frac{x_i x_j W_{ij}}{v(1-\varepsilon_3)} \tag{9}$$

where at least one i or j is an ion and W_{ij} is an ion–ion or ion–molecule interaction parameter. The packing factor ε_3 is calculated by the following formula:

$$\varepsilon_3 = \frac{N\pi}{6}\sum_i \frac{x_i \sigma_i^3}{v} \tag{10}$$

with a summation over all species present, while σ_i is the molecular or ionic diameter, respectively.

The long-range ion–ion interaction term is given by:

$$\left(\frac{A_R}{RT}\right)_{LR} = -\frac{\alpha_{LR}^2}{4\pi}\sum_{ion}\frac{x_{ion} Z_{ion}^2 \Gamma}{1+\Gamma\sigma_{ion}} + \frac{\Gamma^3 v}{3\pi N} \tag{11}$$

The shielding parameter Γ is given implicitly by:

$$4\Gamma^2 = \alpha_{LR}^2 N \sum_{ion}\frac{x_{ion}}{v}\left(\frac{Z_{ion}}{1+\Gamma\sigma_{ion}}\right)^2 \tag{12}$$

$$\alpha_{LR}^2 = \frac{e^2 N}{\varepsilon_0 DRT} \tag{13}$$

where ε_0 is the dielectric permittivity of free space. The dielectric constant D is calculated according to:

$$D = 1 + (D_s - 1)\left(\frac{1-\varepsilon_3''}{1+\varepsilon_3''/2}\right) \tag{14}$$

In this equation ε_3'' is equal to ε_3 as defined in Eq. (10) above; however, the summation is only one for the ions present in the system!

The solvent dielectric constant is given by:

$$D_s = \frac{\sum x_{mol} D_{mol}}{\sum x_{mol}} \tag{15}$$

The summation is only carried out for the molecular pure components present. The pure component dielectric constant is assumed to be temperature dependent (Eq. (16)). No interaction parameters are necessary for the calculation of the dielectric constant.

$$D_i = d^{(0)} + \frac{d^{(1)}}{T} + d^{(2)}T + d^{(3)}T^2 + d^{(4)}T^3 \tag{16}$$

In the above-described model the standard state of the long-range (LR) term is not equal to the standard state of the other terms (RF, SR1 and SR2) of the equation of state. The following standard states are used in the model:

- Ionic standard state in the solvent mixture at unit mole fraction and the system temperature and pressure (for LR term)
- Ideal gas state at unit mole fraction and system temperature and 1 bar (for RF, SR1 and SR2 term)

To prevent this model discrepancy an additional term is added to the equation of state (Born term). This Born term is given by the equation below:

$$\left(\frac{A_R}{RT}\right)_{BORN} = \frac{Ne^2}{4\pi\varepsilon_0 RT}\left(\frac{1}{D_s}-1\right)\sum_i \frac{x_i Z_i^2}{\sigma_i^*} \tag{17}$$

In this work (as in previous work by Fürst and Renon [9]) only the interactions between cations and molecules (W_{cm}) and cations and anions (W_{ca}) were taken into account. Other interactions were not incorporated due to the repulsive forces of anion–anion (W_{aa}) and cation–cation (W_{cc}) interactions and due to lower solvation of anions (W_{am}) as compared to cations (W_{cm}). In this model it is assumed that the ionic binary interaction parameter (W_{ij}) is not temperature dependent.

2.5. Chemical reactions

An alkanolamine-acid gas system is a reactive absorption system, so chemical reactions have to be incorporated in the model. For the CO_2–MDEA–H_2O–CH_4 system, the following

Table 2
Parameters for calculation of chemical equilibrium constants of system CO_2–MDEA–H_2O

Reaction	A	B	C	T (K)	Reference
K_1	132.899	−13445.9	−22.4773	273–498	Posey and Rochelle [13]
K_2	231.465	−12092.1	−36.7816	273–498	Posey and Rochelle [13]
K_3	216.049	−12431.7	−35.4819	273–498	Posey and Rochelle [13]
K_4	−77.262	−1116.5	10.06	278–423	Huttenhuis et al. [15]

chemical reactions will take place:

$$\text{Water dissociation}: \quad 2H_2O \overset{K_1}{\longleftrightarrow} H_3O^+ + OH^-$$

$$\text{Bicarbonate formation}: \quad 2H_2O + CO_2 \overset{K_2}{\longleftrightarrow} HCO_3^- + H_3O^+$$

$$\text{Carbonate formation}: \quad H_2O + HCO_3^- \overset{K_3}{\longleftrightarrow} CO_3^{2-} + H_3O^+$$

$$\text{MDEA protonation}: \quad H_2O + MDEAH^+ \overset{K_4}{\longleftrightarrow} MDEA + H_3O^+$$

The equilibrium constants (based on mole fractions) of these reactions were correlated by the following equation:

$$\ln K_x = A + \frac{B}{T} + C \ln T \tag{18}$$

The relevant parameters for the equilibrium constants as used in the model are given in Table 2

K_1, K_2, K_3 as used by Posey and Rochelle [13] were compared with the chemical equilibrium constants as used by Kamps et al. [16] and differences between these two are negligible. K_4 has been compiled by Huttenhuis et al. [15] from experiments carried out by different research groups.

In this work all chemical equilibrium constants are defined in the mole fraction scale with as reference state infinite dilution in water for all species. Now all the relevant and required equations and parameters, respectively, are specified and the model can be finalized. In the model the amount of H_3O^+ is neglected, since at low to moderate loadings, the solution is alkaline. The mole fraction in the gas and liquid phase of the following species will be calculated in the model: H_2O, OH^-, CO_2, HCO_3^-, CO_3^{2-}, MDEA, $MDEAH^+$ and CH_4.

3. Model development

3.1. Former work

As described in our previous paper (Huttenhuis et al. [15]) the agreement between the original model of Solbraa [7] and newly determined experimental data was not satisfactory. Therefore modifications to the original EOS model of Solbraa [7] were carried out:

- The experimental database used for the determination of the ionic interaction parameter of $MDEAH^+$ with the other species in the system was critically reviewed and updated.
- The dissociation constant of MDEA of the model was changed, because the constant used previously appeared to be not correct compared with the experimental determined equilibrium constants in the literature.

Moreover, it was also concluded (Huttenhuis et al. [15]) that the physical solubility of the CO_2 in the liquid phase, as calculated by the model, was not inline with the experimental data.

For a quantitative comparison of the model with the experimental data the average absolute deviation (AAD) and BIAS-deviation are used and they are given below:

$$\text{AAD} = \frac{1}{n}\sum_{i=1}^{n}\left|\frac{y_{i,\text{exp}} - y_{i,\text{calc}}}{y_{i,\text{exp}}}\right| \times 100\%,$$

$$\text{BIAS} = \frac{1}{n}\sum_{i=1}^{n}\frac{y_{i,\text{exp}} - y_{i,\text{calc}}}{y_{i,\text{exp}}} \times 100\%$$

3.2. Chemical reactions

In the model developed by Solbraa [7], the species OH^- and CO_3^{2-} were not taken into account. However, at very low CO_2 liquid loadings (influence of OH^--ions) and higher MDEA concentrations and/or high CO_2 liquid loadings (influence of CO_3^{2-}-ions) these assumptions may lead to erroneous results. Therefore these two species and the relevant interaction parameters were incorporated in the E-EOS model. For the governing reaction equations and their equilibrium constants reference is made to Section 2.5.

3.3. Binary molecular interaction parameters

3.3.1. Overview

Before the quaternary system CO_2–MDEA–H_2O–CH_4 can be simulated, first the following binary systems have to be studied and optimized:

- CO_2–H_2O: The Huron–Vidal binary interaction parameters for this system were found by fitting the parameters to experimental solubility data (222 data points) of CO_2 in water. This work was carried out by Solbraa [7].
- H_2O–MDEA: In Solbraa's original model 25 freezing point data of Chang et al. [17] have been used to determine the Huron–Vidal interaction parameters. In this work this experimental database was extended and three additional literature sources have been added. New Huron–Vidal interaction parameters were determined with the changed database.
- CO_2–MDEA: In Solbraa's original model the Huron–Vidal interaction parameters were determined by fitting them

Table 3
Model predictions compared with experimental data for the MDEA–H_2O system

Reference	AAD [%]	
	Solbraa's model	This work
Chang at al. [17]	1.5	.25
Xu et al. [20]	2.5	3.1
Voutsas at al. [21]	7.4	3.3
Posey [14]	37.3	4.0

together with the ionic interaction parameters to ternary reactive solubility data. Huttenhuis et al. [15] concluded that the calculated physical solubility of CO_2 in MDEA did not agree with experimental data, so the binary interaction parameter of this system was critically re-evaluated.

- CH_4–CO_2: van der Waals mixing rule was used for this non-polar system. The interaction parameter (k_{ij}) was the same as that used in Solbraa's original model and was taken from Prausnitz et al. [18] and Reid et al. [19].
- CH_4–H_2O: The Huron–Vidal binary interaction parameters for this system were found by fitting the parameters to experimental solubility data (400 data points) of CH_4 in water and water in CH_4. This work was carried out by Solbraa [7].
- CH_4–MDEA: In the Solbraa version of the model this molecular interaction parameter was determined by using it as a fitting parameter (together with the ionic fitting parameter $MDEAH^+$–CH_4) for the ionic system MDEA–H_2O–CO_2–CH_4. In the new approach this interaction parameter is determined from experimental data of the ternary molecular system MDEA–H_2O–CH_4.

3.3.2. H_2O–MDEA

In Solbraa's original model freezing point data (25 data points) of Chang et al. [17] in a relatively small temperature range (262–273 K) have been used to determine the Huron–Vidal interaction parameters. In this work the three additional literature sources have been added so that a higher temperature range was covered (262–460 K), Xu et al. [20] (34 VLE data points), Voutsas et al. [21] (27 VLE data points) and Posey [14] (19 excess heat of mixing data points).

As can be seen in Table 3 the deviations for the water–MDEA system were significantly reduced by the new binary interaction parameters.

In Fig. 2 the calculated activity coefficient for water in the H_2O–MDEA system is compared with the experimental data of Chang et al. [17]. As it can be seen from this figure, the calculated activity coefficient in the new model is significantly improved compared to Solbraa's model, especially for the more concentrated MDEA solutions.

When molecular interaction parameters are fitted to binary data, sometimes multiple sets of parameters are obtained. For the MDEA–H_2O mixture two sets of Huron–Vidal parameters (HV-I and HV-II) were obtained during the regression calculations. In Table 4 the two sets of Huron–Vidal parameters are presented and the thermodynamic consequences are further discussed:

In Figs. 3 and 4 the calculated activity coefficient of H_2O and MDEA is presented for the two different sets of

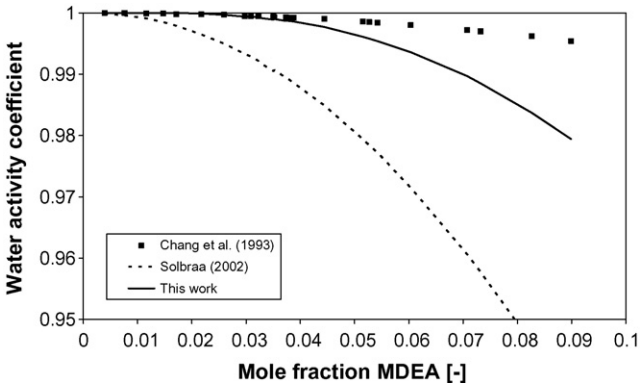

Fig. 2. Activity coefficient of water in a MDEA–H_2O mixture ($263 < T < 273$ K).

Table 4
Two sets of Huron–Vidal parameters for the MDEA–H_2O system

	HV-I	HV-I I
Comp. i	MDEA	MDEA
Comp. j	H_2O	H_2O
α_{ji}	0.208	0.270
$\Delta g'_{ij}$ (J mol^{-1})	−9148	33219
$\Delta g'_{ji}$ (J mol^{-1})	6095	−46531
$\Delta g''_{ij}$ (J mol^{-1} K^{-1})	42.35	−66.84
$\Delta g''_{ji}$ (J mol^{-1} K^{-1})	−49.93	91.29

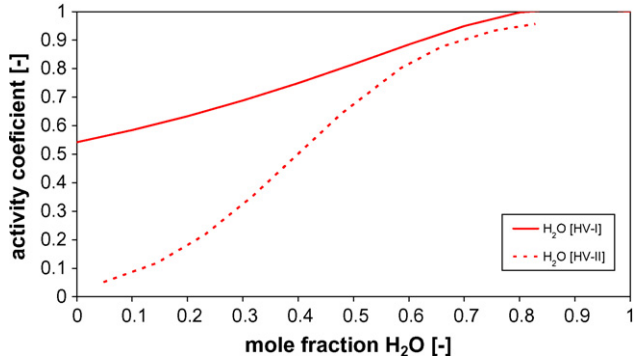

Fig. 3. Calculated activity coefficient of water in a MDEA–H_2O mixture at 40 °C for two different sets of Huron–Vidal parameters (HV-I and HV-II).

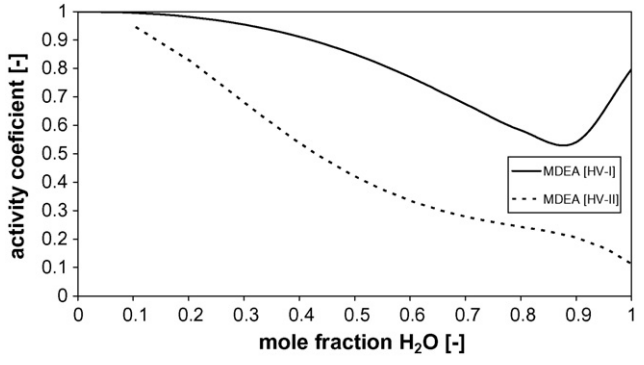

Fig. 4. Calculated activity coefficient of MDEA in a MDEA–H_2O mixture at 40 °C for two different sets of Huron–Vidal parameters (HV-I and HV-II).

Huron–Vidal parameters as function of the mole fraction water at 40 °C.

From Figs. 3 and 4 it can be seen that the behaviour of both MDEA and H_2O activity coefficient is predicted differently for the two sets of parameters. For commercial applications, the used MDEA concentrations results in values for the mole fraction water always above 0.85, so in this concentration range the difference in H_2O activity coefficient predicted by both set of parameters is negligible. The activity coefficient of MDEA, however, is predicted completely different by the two sets of parameters. When the HV-I parameters are used a minimum in MDEA activity coefficient of 0.55 is predicted, while for the HV-II parameters a continuously decreasing activity (with increasing water concentration) is predicted by the model. So in diluted MDEA concentrations the calculated MDEA activity coefficient of the two models differ more than a factor of 5! The minimum in MDEA activity coefficient as function of concentration was also observed by Solbraa [7], Posey [14], Lee [22] and Austgen [23]. However, Austgen concluded that a better model representation of the ternary system (CO_2–MDEA–H_2O) of the model was achieved by adjusting all MDEA–H_2O interaction parameters to zero instead of using the fitted parameters. Austgen, however, could not give a straightforward explanation for this unexpected observation. Contrary to the authors mentioned above, Poplsteinova et al. [24] calculated a continuously decreasing MDEA activity coefficient (with increasing H_2O concentration), comparable with the model using parameters HV-II. In the present study it was decided to use the HV-I parameters in the model, because predictions of the MDEA activity coefficient of this model is in line with most of the other authors. Also the predicted activity coefficient of water at infinite dilution (pure MDEA) of the HV-I model is more in line with the other authors. However, future work is required to generate more experimental data in the commercially important MDEA concentrations range. Different types of data can be determined for the estimation of the Huron–Vidal parameters, however it has been demonstrated by Posey [14] that heat of mixing data and freezing point data are more suitable to predict the binary interaction for MDEA–H_2O system.

3.3.3. CO_2–MDEA

In the original model, the Huron–Vidal interaction parameters were determined by fitting them together with the ionic interaction parameters to ternary solubility data. As already discussed in a previous paper Huttenhuis et al. [15], the physical solubility of CO_2 calculated by the model did not match with experimental data. The physical solubility of CO_2 in MDEA cannot be measured directly, because there are always trace amounts of water present in pure MDEA. These small amounts of water will increase the CO_2 solubility tremendously, due to the chemical reaction which will take place. So for the prediction of the physical solubility in aqueous MDEA, the CO_2–N_2O analogy is widely accepted in the literature. This theory is based on the fact that CO_2 and N_2O are rather similar molecules. The only difference between the molecules is, that N_2O does not chemically (only physically) dissolve in aqueous MDEA. According to the CO_2–N_2O analogy the Henry's constant (physically dissolved CO_2) of CO_2 in aqueous MDEA can be calculated as given by the formula below:

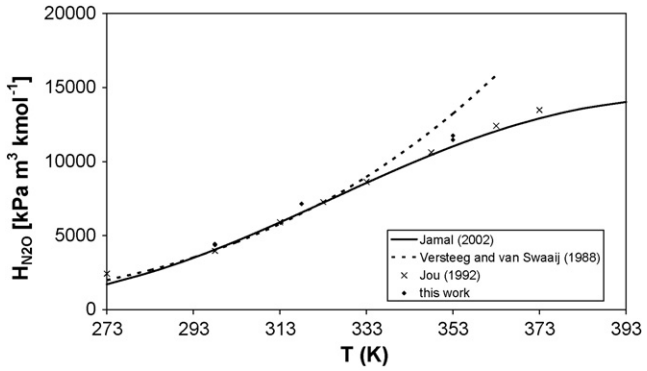

Fig. 5. Henry constant of N_2O in water according relation of Jamal [25], Versteeg and van Swaaij [26], experimental data from Jou et al. [27] and experimental data from this work.

$$H_{CO_2,\,\mathrm{aq.MDEA}} = \frac{H_{CO_2,\mathrm{water}}}{H_{N_2O,\mathrm{water}}} \times H_{N_2O,\mathrm{aq.MDEA}} \tag{19}$$

So the physical solubility of CO_2 in aqueous MDEA can be determined by measuring the solubility of N_2O in water and aqueous MDEA and the solubility of CO_2 in water. In this, indirect, way binary interaction parameters for MDEA–CO_2 can be obtained by using the physical solubility data of CO_2 in aqueous MDEA derived from the equation above and the already determined binary interaction parameters of the MDEA–H_2O and the CO_2–H_2O system. For the solubility of CO_2 and N_2O in water the empirical correlation of Jamal [25] was compared with the relation presented by Versteeg and van Swaaij [26]. The solubility predicted by both relations were comparable until a temperature of approximately 333 K. Above this temperature the Henry constant of N_2O predicted by Versteeg was higher than the Henry constant calculated from the relation of Jamal. Therefore some additional experiments were carried out to verify, which relation was more correct. Experimental data of Jou et al. [27] were also used for the comparison, because in this work experiments where carried out at higher temperatures until 413 K. In Fig. 5 it can be seen that the new experimental data and the work of Jou et al. [27] are more in line with the relation of Jamal, so it was decided to use this correlation for the prediction of N_2O and CO_2 in water.

For the solubility data of N_2O in aqueous MDEA the experimental data of several authors were reviewed and after this review the database as presented in Table 5 was used.

Table 5
Experimental database for solubility of N_2O in aqueous MDEA

Reference	T (K)	MDEA (wt.%)	Number of experiments
Haimour and Sandall [28]	288–308	10–20	12
Jou et al. [29]	298–398	0–40	14
Versteeg and van Swaaij [26]	293–333	4–32	50
Li et al. [30]	303–313	30	3
Pawlak and Zarzycki [31]	293	0–100	9

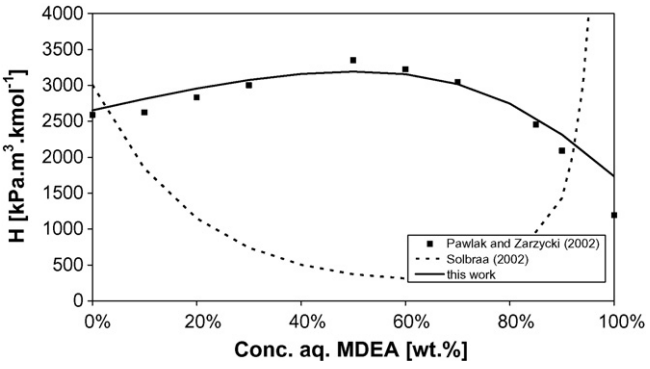

Fig. 6. Physical solubility of CO_2 in aqueous MDEA at 293 K.

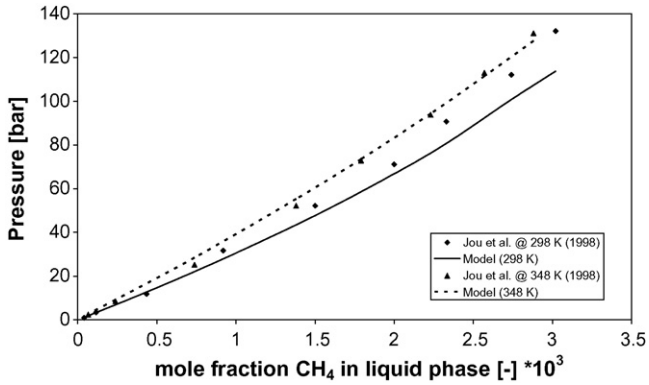

Fig. 7. Physical solubility of methane in aqueous 3 M MDEA.

The available volumetric data as specified above must be converted from volumetric to molar units, so the density of the solutions should be known. Therefore the correlation as presented by Al-Ghawas et al. [32] was used.

With the above set of experimental data and correlations, new Huron–Vidal interaction parameters were determined for the CO_2–MDEA binary system and the physical solubility of CO_2 in aqueous MDEA was calculated and compared with the results of the original model and the experimental results of Pawlak and Zarzycki [31]. In Fig. 6 the results can be seen at 293 K and from this figure it can be concluded that the accuracy of the model is improved significantly with respect to the physical solubility of CO_2 in aqueous MDEA.

All solubility data of N_2O in aqueous MDEA from the experimental database (Table 5) were compared with results of the updated model. AAD and BIAS-deviation were, respectively, 2.7 and 0.2%.

3.3.4. CH_4–MDEA

In the original model of Solbraa [7] both the molecular interaction parameter (CH_4–MDEA) and the ionic interaction parameter (CH_4–$MDEAH^+$) were determined by regressing the model to experimental data of Addicks et al. [33] for the quaternary reactive system (CO_2–MDEA–H_2O–CH_4). In this way two fitting parameters were determined by fitting them to one set of dependent experimental data. In this work a more sound fundamental approach is used. The molecular interaction parameter (k_{ij}) for MDEA–CH_4 is determined by fitting the EOS model with a van der Waals mixing rule with experimental data for the molecular system CH_4–MDEA–H_2O (Jou et al. [34]). Because the CH_4–H_2O and MDEA–H_2O binary interaction parameters were already determined, the CH_4–MDEA parameter can be determined by regressing to the available experimental data. Jou et al. [34] determined the physical solubility of CH_4 in a 3 M aqueous MDEA solution in the temperature interval 298–403 °C. In total 44 experiments were carried out. When the experimental data of Jou et al. [34] were compared with the model total AAD and BIAS-deviation were, respectively, 10.5 and 2.2%. In Fig. 7 the model results are compared with the experimental data at 298 and 348 K, respectively.

3.3.5. Summary

In the above paragraphs all binary molecular interactions which are applicable in the MDEA–H_2O–CO_2–CH_4 system were discussed. In Table 6 the determined interaction parameters are presented.

3.4. Binary ionic interaction parameters

3.4.1. Ionic interaction parameters in MDEA–H_2O–CO_2 system

For the development of the electrolyte part of the EOS model the ionic interaction parameters (W_{ij}) have to be determined. As mentioned in Section 2.4, only the cation–molecule and the cation–anion interactions parameters have to be determined. For the ternary system MDEA–CO_2–H_2O the interaction of $MDEAH^+$-ion with MDEA, H_2O, OH^-, CO_2, HCO_3^- and CO_3^{2-} should be determined. Because the concentration of OH^--ions in the system is normally very low, the $MDEAH^+$–OH^- binary interaction parameter was not fitted but estimated by the correlation given by Fürst and Renon [9]. So the remaining five fitting parameters were determined via the experimental VLE-database for the ternary system MDEA–CO_2–H_2O. It must be noted, however, that the experimental database as used by Solbraa [7] was adapted significantly. A detailed discussion of these changes is given by Huttenhuis et al. [15].

The experimental database as used for the determination of $MDEAH^+$-interaction parameters is presented in Table 7.

The database for the determination of the $MDEAH^+$-interaction parameters consisted of 283 data points. When the distribution of process conditions of this database is studied the following conclusions can be drawn:

- Most of the experimental data (>30% of total experiments) were determined at conditions where the CO_2 loading is lower than 0.1 mol CO_2/mol amine).
- Most of the experimental data were determined at 313 and 373 K (respectively 27 and 17% of the total experiments)
- Most of the experimental data were determined at 25 and 30 wt.% MDEA (both 30% of total experiments)

When the new binary interaction parameters were determined the model results were compared with the experimental database

Table 6
Molecular interaction parameters

Comp. i	CO_2	CO_2	CO_2	MDEA	MDEA	H_2O
Comp. j	MDEA	H_2O	CH_4	H_2O	CH_4	CH_4
k_{ij}			0.096		0.600	
α_{ji}	−0.786	0.030		0.208		0.150
$\Delta g'_{ij}$ (J mol^{-1})	4101	30146		−9148		−1028
$\Delta g'_{ji}$ (J mol^{-1})	2205	−18634		6095		40532
$\Delta g''_{ij}$ (J mol^{-1} K^{-1})	−4.01	32.53		42.35		17.40
$\Delta g''_{ji}$ (J mol^{-1} K^{-1})	−5.68	−26.30		−49.93		−54.45

Table 7
Literature references used for the fitting of the ionic parameters of the MDEA–CO_2–H_2O system

Ref.	MDEA conc. (wt.%)	Temperature (K)	Liquid loading (mol CO_2/mol amine)	Number of points
Lemoine et al. [35]	23.6	298	0.02–0.26	13
Austgen and Rochelle [36]	23.4	313	0.006–0.65	14
Kuranov et al. [37]	19.2	313	1.56–2.46	9
	18.8	313, 333, 373, 413	0.36–2.62	32
	32.1	313, 333, 373, 393, 413	0.41–4.46	40
Rho et al. [38]	5	323	0.24–0.68	7
	20.5	323, 348, 373	0.026–0.848	32
	50	323, 348, 373	0.0087–0.385	26
Kamps et al. [16]	32.0	313	0.85–1.24	5
	48.8	393	0.32–0.56	6
Huang and Ng [39]	23	313, 343, 373, 393	0.00334–1.34	28
	50	313, 343, 373, 393	0.00119–1.16	37
Rogers et al. [40]	23	313, 323	0.000591–.1177	20
	50	313	0.00025–0.037	14

as presented in Table 7; The AAD and BIAS-deviation were, respectively, 24 and 8.3%.

3.4.2. Ionic interactions parameters in MDEA–H_2O–CO_2–CH_4 system

For the quaternary system CO_2–MDEA–H_2O–CH_4 four additional interaction parameters must be determined compared to the system without methane, i.e. the MDEA–CH_4 (Section 3.3.4), CO_2–CH_4 (Section 3.3.1), H_2O–CH_4 (Section 3.3.1) parameter and the $MDEAH^+$–CH_4 parameter. The binary molecular interaction parameters (MDEA–CH_4, CO_2–CH_4 and H_2O–CH_4) have already been determined as described in Section 3.3. So only one additional parameter, the $MDEAH^+$–CH_4 interaction parameter, was determined by regressing the model with experimental VLE data of Addicks et al. [33]. Addicks measured the CO_2 and CH_4 solubility in aqueous MDEA. In total 31 experimental data points were used for the parameter fitting. When the model was fitted to the experimental data of Addicks et al. [33]; the AAD and BIAS were 35 and 22%, respectively, for the partial pressures of CO_2 and 21.5 and −2.8% for the total pressure. Unfortunately, the data of Addicks could not be compared with experimental data from other authors, because this information is unique in its kind.

In Table 8 the ionic interaction parameters are presented.

4. Modeling results

4.1. Ternary system CO_2–MDEA–H_2O

The model CO_2–MDEA–H_2O has been validated with the experimental database for this ternary system. As described in Section 3.4 the AAD and BIAS were 24 and 8.3%, respectively. In Fig. 8, the parity plot with the experimental database of Table 7 is presented for different liquid loadings.

From this figure it can concluded that at low loadings, the partial pressure seems to be somewhat under predicted by the model. When looking to the data at a CO_2 partial pressure of approximately 1 kPa, it can be seen that the predictions for the higher liquid loadings (0.1–1) (at equal partial pressure) are relatively better than the predictions at low liquid loadings (0.01–0.1). So, it seems that the quality of the experimental data at low liquid loadings is more scattered compared with data at higher liquid loadings. In Fig. 9 the experimental data, used for the regression

Table 8
Ionic interaction parameters

Comp. i	$MDEAH^+$	$MDEAH^+$	$MDEAH^+$	$MDEAH^+$	$MDEAH^+$	$MDEAH^+$
Comp. j	CO_2	H_2O	MDEA	HCO_3^-	CO_3^{2-}	CH_4
W_{ij} (m^3 mol^{-1})	2.48E − 04	4.09E − 04	1.95E − 03	−1.29E − 04	−3.58E − 04	4.93E − 04

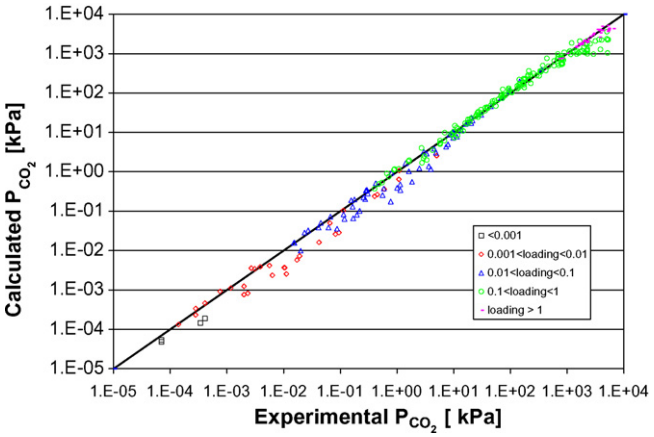

Fig. 8. Parity plot for different liquid loadings (mol CO_2/mol amine).

of parameters of the present E-EOS model is compared for the different authors.

In Table 9 the results of this analysis are presented. Also the model predictions at different temperatures and different MDEA concentrations are presented in Table 9.

From Table 9 it can be concluded that model predictions are good when the liquid loading is above 0.1 mol CO_2/mol amine, because the BIAS-deviation in this area is only +1%. For low loadings (<0.1 mol/mol) the model is always under predicting the CO_2 partial pressure; BIAS-deviation in this area is more than +20% and even more than +30% for liquid loadings below 0.01 mol/mol. A relation between temperature and model predictions cannot be seen clearly. BIAS and AAD deviation are not changing systematically with temperature. The model predictions for MDEA concentration between 20–24% are very good (BIAS = −1%). However, at lower and higher MDEA concentrations the match between model results and experimental data is worse. When looking to the influence of the author on the model predictions it can be concluded that the match with experimental data of Austgen and Rochelle [36] and Kuranov et al. [37] are rather good, with respect to BIAS-deviation; It must be noted, however, that Kuranov did not measure solubility data at low liquid loadings; only high loading data were measured.

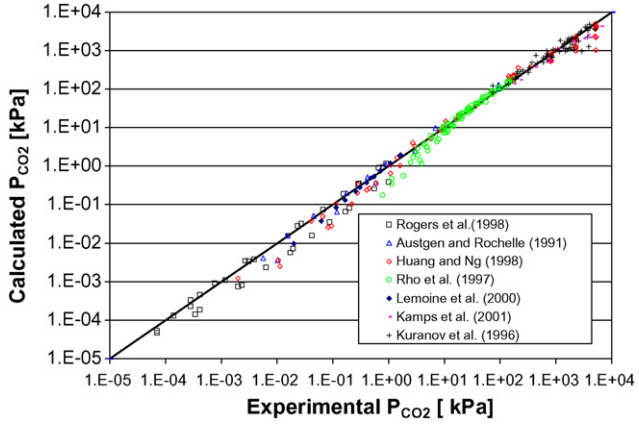

Fig. 9. Parity plot for different authors.

Table 9
BIAS (left column) and AAD deviation (right column) (%) for the experimental data points as function of liquid loading, temperature, MDEA concentration and author; number of experimental data points is given between brackets

Liquid loading [mol CO_2/mol amine]	<0.001 (6)		0.001–0.01 (30)		0.01–0.1 (61)		0.1–1 (153)		>1 (33)	
	28	28	32	38	17	28	1	22	1	11
Temperature (K)	298–313 (100)		323–333 (49)		343–353 (48)		373–393 (86)			
	9	25	3	19	9	19	10	27		
Concentration MDEA [wt.%]	5 (21)		20–24 (135)		32 (5)		47–50 (122)			
	19	22	−1	17	27	27	16	31		
Author	Lemoine [35] (13)		Austgen [36] (14)		Rho [38] (19)		Huang [39] (65)		Rogers [40] (34)		Kamps [16] (14)		Kuranov [37] (64)	
	9	17	0	28	7	19	12	27	17	43	23	25	0	20

As it can be concluded from Table 9, Figs. 8 and 9, the electrolyte equation of state model used in this work, gives an under-prediction of the partial pressure CO_2, i.e. an over-prediction of the gas solubility in the low loading area. This observation was also reported by Fürst and Planche [6], Austgen and Rochelle [36] and Weiland et al. [41]. It must be noted that the models used by these authors were different, so it is not clear at this state to determine exactly the phenomena that cause these under-predictions.

Generally, the spread in experimental determined solubility is much higher at lower loadings (<0.1), compared with the higher liquid loadings. So apparently the experimental accuracy in this loading range is substantially lower compared with the higher liquid loadings. In order to take this inaccuracy at lower liquid loadings into account in the presently developed E-EOS model, these were omitted from the database. Next new ionic interaction parameters (W_{ij}) were determined with the reduced experimental database excluding the data at loadings below 0.1. From an analysis of the results it was concluded that on average the model was not improved significantly. Still there was a large under-prediction of the CO_2 partial pressure. Therefore the model with the ionic parameters determined with the whole database as presented in Table 7 was used for further study. It can also be concluded that at lower liquid loadings a need exists for better and more reliable experimental data.

As mentioned before one of the major advantages of a rigorous fundamentally more correct electrolyte E-EOS model compared to the more simplified models, is that the distribution of the different species present in the liquid phase can be calculated more accurately. Therefore the speciation calculated by the present model was compared with experimentally determined speciation carried out by Poplsteinova et al. [24]. Poplsteinova et al. measured the molecular and ionic concentrations at equilibrium conditions for the absorption of CO_2 in different amine solutions with a NMR technique. In Fig. 10 experimental data of Poplsteinova et al. [24] are compared with the E-EOS model results.

From Figs. 10 and 11 it can be concluded that the speciation calculations of the present model are well in line with the experimental data of Poplsteinova et al. [24]. At higher liquid loadings (>0.8 mol/mol), a small over-prediction of $MDEAH^+$ (Fig. 10)

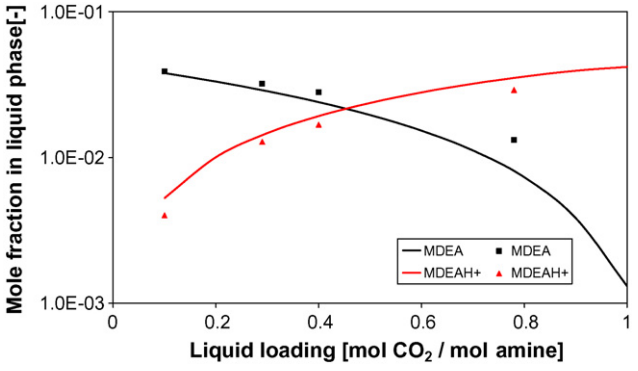

Fig. 10. Speciation of MDEA species in 23 wt.% MDEA at 293 K calculated by the E-EOS model (lines) compared with experimental values of Poplsteinova et al. [24] (points).

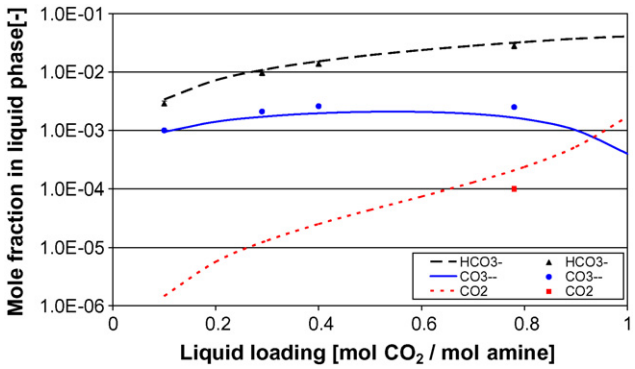

Fig. 11. Speciation of CO_2 species in 23 wt.% MDEA at 293 K calculated by the E-EOS model (lines) compared with experimental values of Poplsteinova et al. [24] (points).

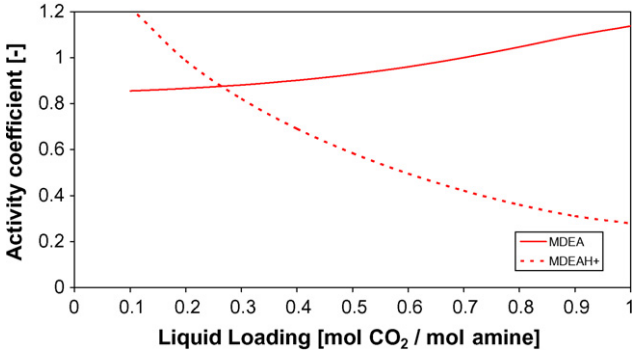

Fig. 12. Activity coefficient of MDEA species in 23 wt.% MDEA at 293 K calculated by the E-EOS model.

and HCO_3^- and an under-prediction of CO_3^{2-} (Fig. 11) is seen; however the deviations are relatively small.

In Figs. 12 and 13 the activity coefficients as calculated by the E-EOS are presented for the various species at different liquid loadings. From this figure it can be seen that the activity of the $MDEAH^+$ (Fig. 12) is decreasing and the activity of HCO_3^- (Fig. 13) is increasing with increasing CO_2 liquid loading. The change in activity coefficient for the other species with liquid loading is relatively small. However, it must be concluded that for all species, excluding CO_2, the activity coefficients are deviating substantially from unity. It has been proven that the reaction constant based on concentrations is not a true constant

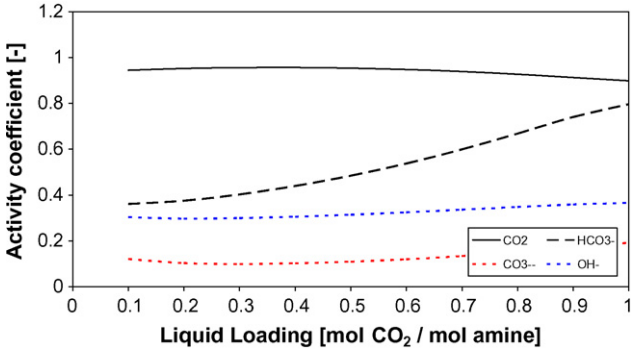

Fig. 13. Activity coefficient of CO_2 species in 23 wt.% MDEA at 293 K calculated by the E-EOS model.

Table 10
Model results for system CO_2–MDEA–H_2O–CH_4

Reference	Number of points	BIAS (%)	AAD (%)
Addicks et al. [33]	31	22	35
Huttenhuis et al. [15]	51	16	30

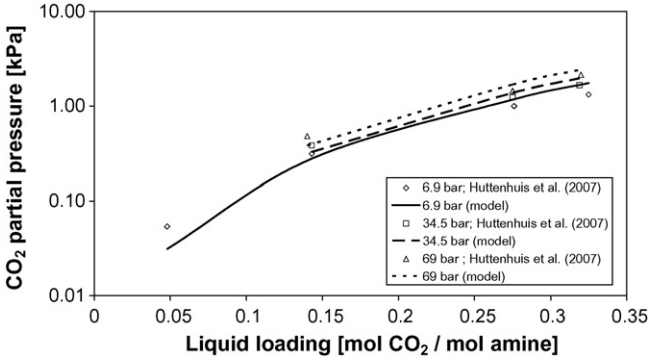

Fig. 14. Solubility of CO_2 in 35 wt.% MDEA at 10 °C.

because it is dependent on the other non-reactive species present in the liquid phase. However when the reaction rate constant is based on activities instead of concentrations a "true" constant can be derived and all non-idealities of the system are incorporated in the activities of the reactive component. For example, the influence of the counter-ion (Li, Na and K) on the reaction between the hydroxide ion and carbon dioxide has been studied experimentally by Haubrock et al. [42].

4.2. Quaternary system CO_2–MDEA–H_2O–CH_4

The system CO_2–MDEA–H_2O–CH_4 has been validated with the experimental data from Addicks et al. [33] and the experimental data determined by Huttenhuis et al. [15]. Results are given in Table 10.

As can be concluded from Table 10, the E-EOS model is under-predicting (BIAS > 0) the CO_2 partial pressure for both authors. In Figs. 14 and 15 the results of the E-EOS model are compared with the experimental data for two different amine concentrations (35 wt.% and 50 wt.%). As it can be seen from this figures, the prediction for the higher (50 wt.%) MDEA

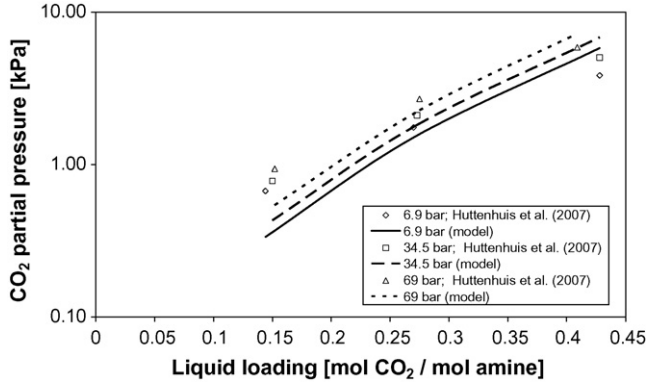

Fig. 15. Solubility of CO_2 in 50 wt.% MDEA at 10 °C.

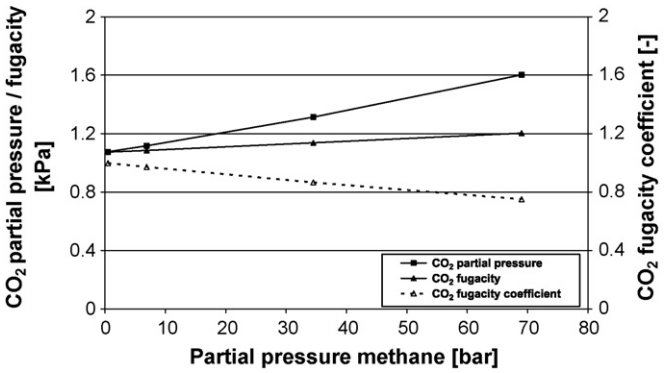

Fig. 16. Partial pressure, fugacity and fugacity coefficient of CO_2 in 35 wt.% MDEA at 25 °C at a liquid loading of 0.1 mol CO_2/mol amine.

concentration (BIAS = +25.2%) is poorer, than the model predictions for 35 wt.% MDEA (BIAS = +5.5%). This was also seen for the solubility data of the ternary system (CO_2–MDEA–H_2O). As it can be seen from Table 9, the model predictions with MDEA concentrations of 20–24 wt.% (BIAS = −1%) are much better than the predictions for 47–50 wt.% (BIAS = 16%). A possible explanation for this different behaviour is that the CO_2–N_2O analogy used for the determination of the Huron–Vidal parameters of the CO_2–MDEA system might not be applicable for the higher MDEA concentrations. The influence of methane on the solubility of CO_2 in the liquid phase is predicted correctly by the model. As can be seen from both the model and from the experiments, the CO_2 solubility decreases with increasing partial pressure of methane. Other thermodynamic models like Kent–Eisenberg [2], Debye-Hückel [43] and NRTL [44] model do not have this effect of inert gas and/or system pressure on the solubility, included in the same way for liquid and vapour phase.

In Fig. 16 the partial pressure, fugacity and fugacity coefficient of CO_2 are presented graphically as function of partial pressure methane. From this graph it can be seen that the CO_2 partial pressure is increasing (which is equivalent to decreasing CO_2 solubility) with the partial pressure methane at constant CO_2 liquid loadings. However, the CO_2 fugacity, remains fairly constant at the different methane partial pressures.

From Fig. 16 it can be concluded that the decreasing solubility of CO_2 at conditions with higher partial pressures of methane can be attributed by a decreasing fugacity coefficient of CO_2.

5. Conclusions

In the present study an electrolyte equation of state model as developed by Solbraa [7] was systematically reviewed, optimized and validated with experimental data for the system MDEA–H_2O–CO_2–CH_4. With this model excellent results were obtained and a lot of information can be derived. It has been proven (experimentally and by the model) that both the system pressure and/or partial pressure methane, respectively have a significantly effect on the solubility of CO_2 in aqueous MDEA solutions. A decrease in CO_2 solubility has been observed, when the partial pressure of methane is increased. As the partial pres-

sure CO_2 is increasing with the methane partial pressure, the CO_2 fugacity is less dependent of the methane partial pressure. So based on fugacities, it can be concluded that the CO_2 solubility seems only slightly dependent of methane partial pressure. At the moment it is not clear if this decrease in CO_2 solubility is caused by the increase in pressure of the system or that the additional methane is responsible for this phenomenon. Model predictions in general are in line with experimental data. At low CO_2 liquid loadings the predicted CO_2 partial pressure is lower than the experimental partial pressure. This conclusion is in line with most other authors. At lower MDEA concentrations (<30 wt.%) model predictions are better than at high MDEA concentrations. This phenomena may be caused by the fact the CO_2–N_2O analogy as used in this work is not applicable in more concentrated amine solutions.

List of symbols

a	attractive term in equation of state (J m^3/mol)
A	Helmholtz energy (J)
AAD	absolute average deviation (%)
b	repulsive term in equation of state (m^3 mol^{-1})
BIAS	mean BIAS-deviation (%)
d	coefficients for dielectric constant
D	dielectric constant
DEA	diethanol amine
e	electron charge (1.60219×10^{-19}) (C)
g	interaction parameter in Huron–Vidal mixing rule (J m^{-3})
H	Henry's coefficient [kPa m^3 kmol^{-1}]
k	binary (molecular) interaction parameter
MDEA	*N*-Methyldiethanolamine
K	chemical equilibrium constant
n	mole number (mol)
N	Avogadro's constant (6.02205×10^{23}) (mol^{-1})
p_1, p_2, p_3	polarity parameters
P	(partial) pressure (Pa)
R	gas constant (J mol^{-1} K^{-1})
T	temperature (K)
v	molar volume (m^3/mol)
W	binary ionic interaction parameter (m^3 mol^{-1})
x	liquid mole fraction
Z	charge

Greek letters

α	binary non-randomness parameter in Huron–Vidal mixing rule
α	correction factor for attraction parameter A^{SR}
α_{LR}	long-range parameter in ionic interaction term (m)
γ	activity coefficient
Γ	shielding parameter (m^{-1})
ε_0	vacuum electric permittivity (C^2 J^{-1} m^{-1})
ε_3	packing factor
σ	ionic/molecular diameter (m)
τ	energy parameter in Huron–Vidal mixing rule
ω	acentric factor

Sub/superscripts

∞	infinite dilution
a	anion
aq.	aqueous
c	cation
C	critical
calc	calculated by model
exp	experiments
i,*j*	index
L	liquid phase
m	molecular
mix	mixture
R	reduced/residual
S	solvent
V	vapour phase

References

[1] J. Schwarzentruber, H. Renon, S. Watanasiri, Fluid Phase Equilib. 52 (1989) 127–134.
[2] R.L. Kent, B. Eisenberg, Hydrocarbon Process. 55 (1976) 87–90.
[3] R.D. Deshmukh, A.E. Mather, Chem. Eng. Sci. 36 (1981) 355–362.
[4] S.L. Clegg, K.S. Pitzer, J. Phys. Chem. 96 (1992) 3513–3520.
[5] D.M. Austgen, G.T. Rochelle, X. Peng, C.C. Chen, Ind. Eng Chem. Res. 28 (1989) 1060–1073.
[6] W. Fürst, H. Planche, Entropie 202/203 (1997) 31–35.
[7] E. Solbraa, Equilibrium and non-equilibrium thermodynamics of natural gas processing, Ph.D. Thesis, Norwegian University of Science and Technology, 2002.
[8] P.W.J. Derks, H.B.S. Dijkstra, J.A. Hogendoorn, G.F. Versteeg, AIChE J. 51 (2005) 2311–2327.
[9] W. Fürst, H. Renon, AIChE J. 39 (1993) 335–343.
[10] P.J.G. Huttenhuis, G.F. Versteeg, Poceedings of the Laurance Reid Gas Conditioning Conference, Norman, OK, USA, 2006.
[11] M.J. Huron, J. Vidal, Fluid Phase Equilib. 3 (1979) 255–271.
[12] G. Vallée, P. Maugin, S. Jullian, W. Fürst, Ind. Eng. Chem. Res. 38 (1999) 3473–3480.
[13] M.L. Posey, G.T. Rochelle, Ind. Eng. Chem. Res. 36 (1997) 3944–3953.
[14] M.L. Posey, Thermodynamic model for acid gas loaded aqueous alkanolamine solutions, Ph.D. Thesis, University of Texas, 1996.
[15] P.J.G. Huttenhuis, N.J. Agrawal, J.A. Hogendoorn, G.F. Versteeg, J. Petrol. Sci. Eng. 55 (2007) 122–134.
[16] Á. Pérez-Salado Kamps, A. Balaban, M. Jödecke, G. Kuranov, N. Smirnova, G. Maurer, Ind. Eng. Chem. Res. 40 (2001) 696–706.
[17] H.T. Chang, M. Posey, G.T. Rochelle, Ind. Eng. Chem. Res. 32 (1993) 2324–2335.
[18] J.M. Prausnitz, R.N. Lichtentahler, E.G. de Azevedo, Molecular Thermodynamics of Fluid-Phase Equilibrium, Third ed., Prentice Hall Int., 1999.
[19] R.C. Reid, J.M. Prausnitz, B.E. Poling, The Properties of Gases and Liquids, fourth ed., McGraw-Hill, 1988.
[20] S. Xu, S. Qing, Z. Zhen, C. Zhang, J.J. Carroll, Fluid Phase Equilib. 67 (1991) 197–201.
[21] E. Voutsas, A. Vrachnos, K. Magoulasm, Fluid Phase Equilib. 224 (2004) 193–197.
[22] L.-J.B. Lee, A vapor–liquid equilibrium model for natural gas sweetening process, Ph.D. Thesis, Oklahoma State University, 1996.
[23] D.M. Austgen, A model of vapor–liquid equilibria for acid gas–alkanolamine–water systems, Ph.D. Thesis, University of Texas, 1989.
[24] J. Poplsteinova Jacobsen, J. Krane, H.F. Svendsen, Ind. Eng. Chem. Res. 44 (2005) 9894–9903.
[25] A. Jamal, Absorption and desorption of carbon dioxide and carbon monoxide in alkanolamine systems, Ph.D. Thesis, University of British Columbia, 2002.

[26] G.F. Versteeg, W.P.W. van Swaaij, J. Chem. Eng. Data 32 (1988) 29–34.
[27] F.-Y. Jou, J.J. Carroll, A.E. Mather, F.D. Otto, Z. Phys. Chem. 177 (1992) 225–239.
[28] N. Haimour, O.C. Sandall, Chem. Eng. Sci. 39 (1984) 1791–1796.
[29] F.-Y. Jou, J.J. Carroll, A.E. Mather, F.D. Otto, 9th IUPAC Conference on Chemical Thermodynamics, Lisbon, 1986.
[30] Y.G. Li, A.E. Mather, Fluid Phase Equlib. 96 (1994) 119–142.
[31] H.K. Pawlak, R. Zarzycki, J. Chem. Eng. Data 47 (2002) 1506–1509.
[32] H.A. Al-Ghawas, D.P. Hagewiesche, G. Ruiz-Ibanez, O.C. Sandall, J. Chem. Eng. Data 34 (1989) 385–391.
[33] J. Addicks, G.A. Owren, A.O. Fredheim, K. Tangvik, J. Chem. Eng. Data. 47 (2002) 855–860.
[34] F.-Y. Jou, J.J. Carroll, A.E. Mather, F.D. Otto, J. Chem. Eng. Data. 43 (1998) 781–784.
[35] B. Lemoine, Y.-G. Li, R. Cadours, C. Bouallou, D. Richon, Fluid Phase Equilib. 172 (2000) 261–277.
[36] D.M. Austgen, G.T. Rochelle, Ind. Eng. Chem. Res. 30 (1991) 543–555.
[37] G. Kuranov, B. Rumpf, N.A. Smirnova, G. Maurer, Ind. Eng. Chem. Res. 35 (1996) 1959–1966.
[38] S.-W. Rho, K.-P. Yoo, J.S. Lee, S.C. Nam, J.E. Son, B.-M. Min, J. Chem. Data 42 (1997) 1161–1164.
[39] S.H. Huang, H.-J. Ng, GPA Research Report RR-155, 1998.
[40] W.J. Rogers, J.A. Bullin, R.R. Davidson, AIChE J. 44 (1998) 2423–2430.
[41] R.H. Weiland, T. Chakravarty, A.E. Mather, Ind. Eng. Chem. Res. 32 (1993) 1419–1430.
[42] J. Haubrock, J.A. Hogendoorn, G.F. Versteeg, Chem. Eng. Sci. 62 (2007) 5753–5769.
[43] P. Debye, E. Hückel, Phys. Z. 24 (1923) 185.
[44] H. Renon, J.M. Prausnitz, AIChE J. 14 (1968) 135.